Powder metallurgical production of SS316L metallic implant with a hybrid bioactive composed of HA and YSZ: Effect of compaction pressure on morphological, mechanical characteristics and bioactivity properties

Ahmad Farrahnoor^{1,a*}, Mahfuzah Zainudin^{1, b}, Clive Eswood Henry¹, Muhammad Fawwaz Azarudin¹

¹Centre for Mechanical Engineering Studies, Universiti Teknologi MARA, Cawangan Pulau Pinang, Permatang Pauh Campus, 13500 Pulau Pinang, Malaysia

^{a*}farra728@uitm.edu.my, ^bmahfuzah035@uitm.edu.my

Abstract

A novel hybrid bioactive ceramic for metallic implant was developed to achieve strong interfacial bonding and osseointegration. This study investigated the morphological, mechanical characteristics, and bioactivity properties of SS316L/HA/YSZ composite through the powder metallurgy method. Various compaction pressures (200, 300, and 400 MPa) were explored to address the difference in Young's modulus between the implant and human bone. Subsequently, the composites were sintered at 800 °C for 2 h with a heating rate of 10 °C/min. Microstructural and mechanical evaluations were performed using SEM, density, and compressive strength tests, while the bioactivity of the composites was assessed through an immersion test. The findings revealed that lower compaction pressure leads to lower densification, higher porosity, higher compressive strength, lower Young's modulus, and increased apatite deposition. The ideal compaction pressure of 200 MPa was identified, as it aligns with the mechanical and bioactivity qualities required for cortical bone, resulting in a compressive strength of 121.07 MPa, Young's modulus of 31.39 GPa, porosity of 33.29% and denser apatite formation (1.64%).

Keywords: bone implant, apatite, bioactivity, hydroxyapatite, yttria-stabilized zirconia.

1. Introduction

The increasing use of orthopedic implants, especially hip and knee joint replacements for elderly patients, has stimulated interest and concern regarding the long-term effects of the materials employed. Around 10% of adults in Malaysia may require surgery to replace a diseased or injured hip joint with an artificial implant [1]. Metallic implants have emerged as the primary option for those who require bone implant surgery. The high demand for metallic implants is due to their ability to withstand substantial loads, high fatigue resistance, and capability to undergo plastic deformation before failure. These properties are not attainable in pure ceramic or polymeric biomaterials.

The most common metals used to manufacture implants include stainless steel, cobalt-based, and titanium-based alloys. Among these, 316L stainless steel (SS316L) has been used as an implant material for several decades due to its low cost and widespread availability [2]. Furthermore, SS316L has high corrosion resistance, heat resistance, biocompatibility, and good mechanical properties. Despite possessing excellent properties, SS316L has a higher Young's modulus (189-205 GPa) compared to cortical bone (10-40 GPa), leading to the stress-shielding phenomenon [3]. This results in bone resorption around the implant and compromises the reliability (clinical success), causing implant loosening. Approximately 5% to 10% of bone implants can still fail due to various reasons during the five-year post-implantation period [4]. To maintain the patient's quality of life, a metal implant with Young's modulus close to that of cortical bone is required to inhibit bone atrophy and enhance bone remodeling for implants. Apart from that, SS316L is considered bioinert, which complicates its integration with bone tissue and reduces the implant's durability. To address this issue, a strategy involving the incorporation of bioactive ceramics to enhance the bioactivity, like yttria-stabilized zirconia (YSZ) and hydroxyapatite (HA), into SS316L, is employed.

HA is the most widely used bioactive ceramic material in the field of bone regeneration due to its stability, faster simulation in bone formation, reduced healing time, promotes cell attachment and proliferation of a variety of cells, including fibroblasts, osteoblasts, and periodontal ligament cells [5]. A. Farrahnoor and H. Zuhailawati [6] suggested that 10 wt.% HA is the optimum amount for enhancement in apatite deposition on metal implant without leading to excessive brittleness. In another study, X. Yin et al. [7] studied the influence of YSZ-coated metal implants. They concluded that YSZ significantly influences decreased inflammatory response due to its excellent tissue attachment features, apatite formation capacity, and biocompatibility compared to bare metal implants. Additionally, improved mechanical properties on implant material have been reported with HA/YSZ coatings compared to bulk HA alone [8], [9].

The production of biomaterials through the powder metallurgy (PM) route offers cost-effectiveness, near-net shape, flexibility and reduces the risk of microstructural inhomogeneity in fabricated composites. The PM process involves three major steps: mixing different powder materials, die compaction, and sintering. PM allows for controlled characteristics, essential for achieving the desired design and creating a dense implant with the desired porosity. Proper compaction of the powder is crucial to form a composite with minimal defects. Uniaxial pressing is the most common method of compaction to form PM components, in which the powder is compressed into a rigid die at pressures ranging from 20 to 700 MPa in a single axial direction using a punch.

An ideal material for implant use should possess adequate mechanical properties and a bioactive surface for bone integration. Moreover, it is important to note that the compressive strength of human cortical bone ranges between 100 and 230 MPa [10], while the range of cortical porosity measurements falls within 1.6 to 46% [11-13]. The main objective of this study was to produce an SS316L composite containing hybrid bioactive component, such as HA/YSZ, using the PM route. The composite was fabricated by applying 200, 300, and 400 MPa compaction pressures. After compaction, the composite green compact is ejected from the hardened steel die and sintered to enhance the composite's properties further. The effects of compaction pressure on the resulting composite's morphological, mechanical characteristics, and bioactivity properties were then evaluated.

2. Materials and Method

2.1 Preparation of SS316L/HA/YSZ composite

The raw materials used were SS316L powder (Sandvik Osprey), HA powder (Sigma Aldrich) and YSZ powder (Sigma Aldrich). SS316L is the matrix in the composite while HA and YSZ are used as reinforcement and bioactive elements. The proportion of the composite was set at 87 wt.% of SS316L, 10 wt.% of HA and 3 wt.% of YSZ. They were weighed using an electronic balance to develop an SS316L/HA/YSZ composite. A high-energy planetary ball mill was used to conduct the experiments. Hardened steel milling balls with a fixed 10:1 ball-to-powder weight ratio (BPR) were placed with the powders. About 3% of polyvinyl alcohol (PVA) was added to prevent agglomeration during milling. Cylindrical specimens of the composite having a 10 mm diameter were prepared by pressing at different pressures (i.e. 200, 300 and 400 MPa). Subsequently, the composites were sintered in a tube furnace under an argon atmosphere. The sintering temperature was set at 800 °C for 2 h with a heating rate of 10 °C/min. Finally, the composites were furnace-cooled to reach room temperature.

2.2 Characterization of SS316L/HA/YSZ composite

The microstructural characterization of composites was performed using scanning electron microscopy (SEM, TM3030 Tabletop Microscope with SwiftED3000). The mechanical properties of the composite, with a thickness and diameter of 10 mm, were evaluated using a compression test conducted on a universal testing machine (Shimadzu AG-IS-50kN) at a crosshead speed of 1 mm/min. The dimensions of the tested composites adhered to the ASTM E9-09 standards. Immersion tests were carried out in Hank's Balanced Salt Solution (HBSS) for four days at 37 °C. Subsequently, the weight gain of the tested composites was determined to calculate the apatite deposition. Meanwhile, the porosities are calculated by Archimedes' method as shown in Eq. (1):

Porosity (%) =
$$100$$
 – relative density (1)

The relative density is calculated based on the theoretical rule of mixture (ROM) as shown in Eq. (2)-(4):

Relative density (%) = Density / Density_{ROM} x
$$100\%$$
 (2)

Density_{ROM} =
$$\rho_{SS316L}$$
 V_{SS316L} + ρ_{HA} V_{HA} + ρ_{YSZ} V_{YSZ} (3)

$$V_{SS316L} + V_{HA} + V_{YSZ} = 1$$
(4)

where ρ_{SS316L} , ρ_{HA} and ρ_{YSZ} represent the density of SS316L, HA and YSZ, respectively, whereas V_{SS316L} , V_{HA} and V_{YSZ} represent the volume fraction of SS316L, HA and YSZ, respectively.

3. Result and Discussion

3.1 Density and porosity measurement

Fig. 1 shows the density and porosity of the SS316L/HA/YSZ composite under different compaction pressures. The experimental density is higher than the theoretical density of SS316L/HA/YSZ composite, which is 4.36 g/cm³. This difference could be attributed to environmental factors and how the experiment is handled. As the compaction pressure increases, the composite's densification also increases, leading to a decrease in porosity. The highest 6.52 g/cm³ density was achieved at 400 MPa, corresponding to the lowest porosity of 23.83%. Conversely, the lowest density of 5.52 g/cm³ was observed at 200 MPa, resulting in the highest porosity of 33.29%. When the compaction pressure is low, insufficient force is applied to the powder particles, leading to less effective particle packing. As a result, voids may form between the particles, resulting in lower densification and higher porosity in the composite. This confirmed the results by K. Essa et al. [14], who reported a remarkable drop in the mechanical properties of the sintered SS316L due to the increased porosity level. On the other hand, applying higher compaction pressure exerts a greater force on the powder particles, enabling better particles with closer contact and making it easier for them to bond during the subsequent sintering process. This minimized the voids between the particles, leading to higher densification. The reduction in porosity is a direct consequence of this enhanced densification. With fewer voids, there is less space for pores to form within the composite, resulting in improved mechanical properties. The results show that dense structures can be achieved when high compaction pressure is used. This agrees with the results presented by M. Gradzka-Dahlke [15]., who fabricated SS316L by powder metallurgy method. They reported that 41, 33, and 26% porosity was obtained at the compaction pressure of 200, 400, and 600 MPa, respectively. The optimal porosity of implant material for ingrowths of new-bone tissues is in the range of 20-30 vol. % [16], [17]. Hence, the data obtained in this study meet the requirements mentioned.

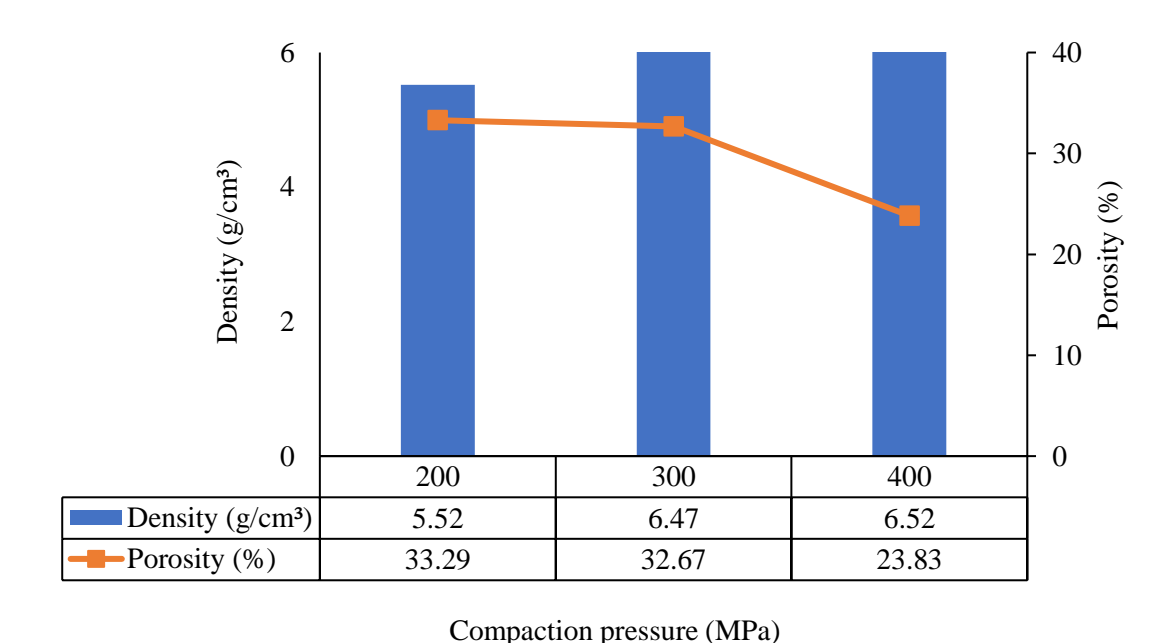


Fig. 1: Density and porosity of SS316L/HA/YSZ composite at different compaction pressure

3.2 Compression test

Fig. 2 shows the correlation between compressive strength and Young's modulus of SS316L/HA/YSZ composite under different compaction pressures. The compressive strength shows a proportional relationship with Young's modulus. The composite exhibited the highest compressive strength of 227.87 MPa at a compaction pressure of 400 MPa, while the lowest compressive strength of 121.07 MPa was observed at 200 MPa. As the compaction pressure increases, the gap between particles reduces, thus minimizing the voids between them. This results in a stronger interfacial bond between the composite particles with fewer interconnected pores. Subsequently, during the sintering process, the particles undergo diffusion mechanisms, improving the composite's strength. Regarding the Young's modulus, the composite exhibited the lowest Young's modulus of 31.39 GPa at 200 MPa, while the highest Young's modulus of 35.67 GPa was achieved at 400 MPa. Simultaneously, the obtained Young's modulus is close to that of cortical bone (10 - 40 MPa) to prevent bone resorption and achieve good bone remodelling. Consequently, Young's modulus of SS316L/HA/YSZ composite is governed by the amount of porosity present in the composite, depending on the increasing compaction pressure. Higher compaction pressure results in lower porosity and higher Young's modulus. When powders are compressed under high pressure, the particles are forced closer together. This results in better packing of the particles, reducing the void spaces between them. The tighter packing reduces the volume of interconnected pores, thus lowering porosity. As porosity decreases, the composite becomes denser and stiffer. The correlation in porosity with compressive strength and Young's modulus agrees with a study performed by W. Zhang et al. [18], who studied the effect of porosity on the mechanical properties of porous stainless steel.

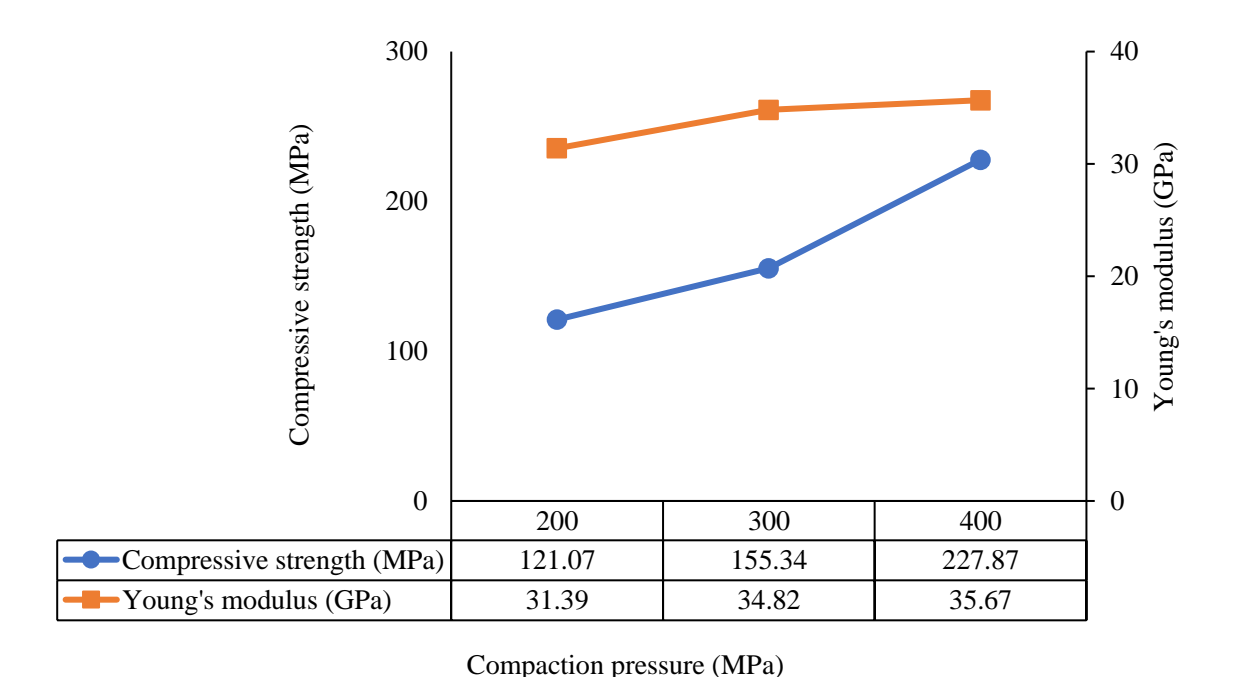
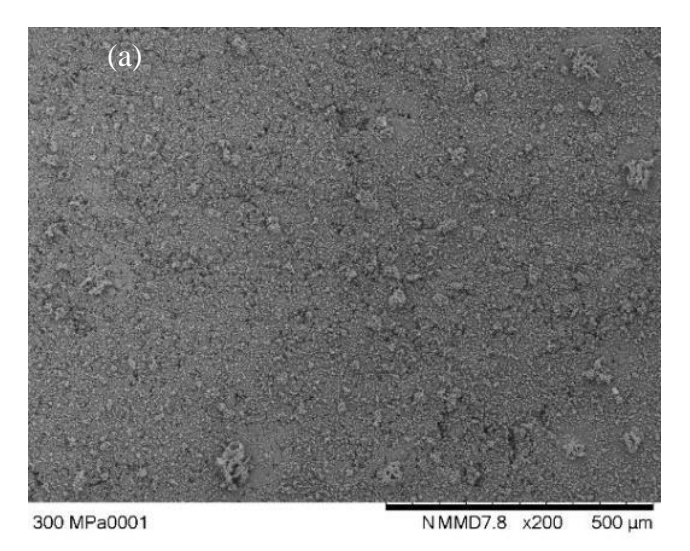


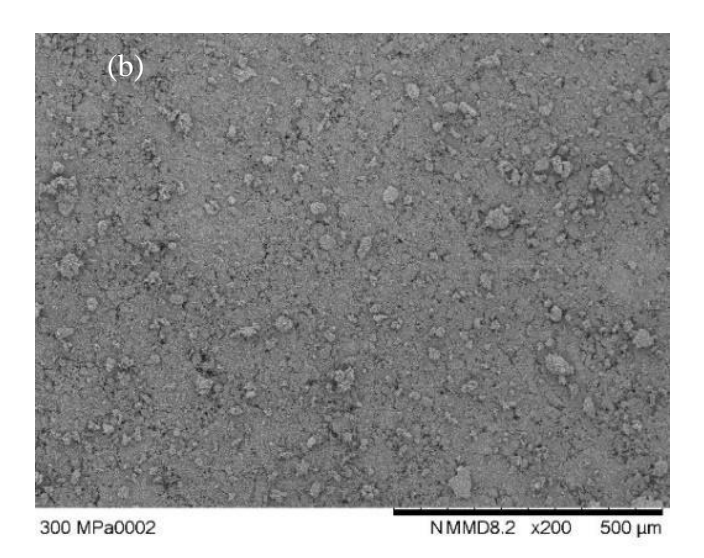
Fig. 2: Mechanical properties of SS316L/HA/YSZ composite at different compaction pressure

3.3 Apatite observation

In order to examine the possibility of SS316L/HA/YSZ composite for implant application, the composites were immersed in HBSS. Fig. 3 shows the surfaces of SS316L/HA/YSZ composite after immersion in HBSS for four days, showing the deposition of apatite crystals on these surfaces. The composite compacted at 200 MPa exhibited the highest degree of apatite coverage, while those compacted at 400 MPa had the lowest. This difference in apatite coverage may be attributed to the porous structure of the composites. J. Zhua et al. [19] reported that porous structures can accelerate the kinetic deposition of apatite when immersed in a physiological solution. A lower compaction pressure resulted in higher porosity in the composite, facilitating denser apatite deposition. The apatite deposition was observed due to the formation of calcium phosphate (CaP) clusters with a high concentration of calcium ions (Ca²⁺) around the pore [20]. It can be concluded that the pores play an important

role in apatite growth. The observed trend in apatite growth is consistent with the weight changes observed in Section 3.4.





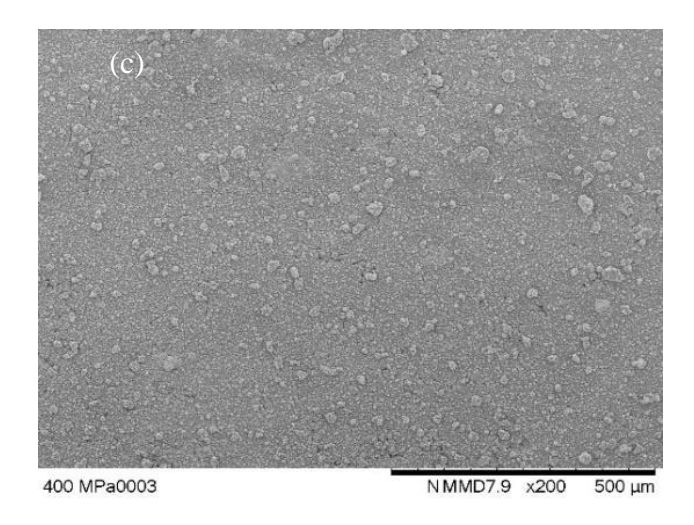
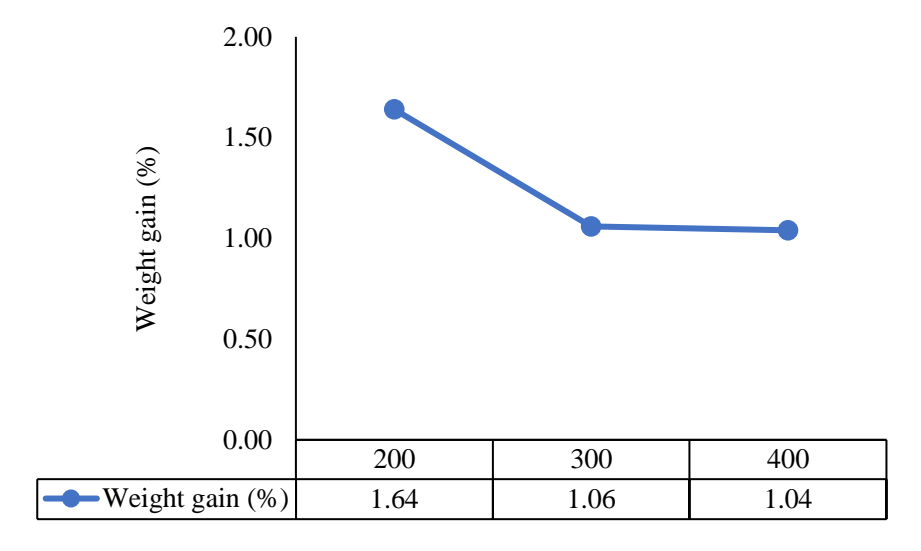


Fig. 3: The SEM images on apatite formation of SS316L/HA/YSZ composite at different compaction pressures: (a) 200 MPa, (b) 300 MPa, and (c) 400 MPa (200 magnification)

Vol. 44 No. 5 (2023)

3.4 Weight gain measurement

The amount of apatite deposited on the surface of the SS316L/HA/YSZ composite is shown in Fig. 4. The observed trend in apatite deposition is directly influenced by the porosity of the composite. The highest weight gain (1.64%) was measured in the composite with a compaction pressure of 200 MPa, while the lowest weight gain (1.04%) was observed at 400 MPa. Apatite formation is more likely to occur at lower compaction pressures due to the increased porosity, which subsequently leads to a higher weight gain after immersion. This is in agreement with similar finding reported by M. Zengdong et al. [21] who discovered that as the porosity of the composite increased, apatite deposition also increased. The higher porosity in the composite provides more open spaces and interconnected voids. When the composite is exposed to HBSS, this physiological solution can penetrate into the voids and access a larger surface area of the composite. Additionally, a larger surface area resulting from higher porosity provides more nucleation sites for apatite formation, increasing the likelihood of apatite crystal growth and deposition on the composite surface.



Compaction pressure (MPa)

Fig. 4 : Deposit weight of apatite on SS316L/HA/YSZ composite surface as a function of compaction pressure

4. Conclusion

The results presented here indicate that the SS316L/HA/YSZ composite can be considered as a potential implant serving under load-bearing conditions. By tuning the compaction pressure within the range of 200 MPa to 400 MPa, the observed apatite deposition may suggest the possibility for new bone formation when using this hybrid bioactive ceramic in metallic implants, while still maintaining acceptable mechanical properties comparable to cortical bone. This new material significantly improves osseointegration and reduces the risk of stress shielding, making it ideal for orthopedic applications operating under load-bearing conditions.

Acknowledgement

This work was supported by MyRA Grant. Project Number: 600-RMC 5/3/GPM (068/2022).

References

- [1] D. Grace, Weak knees & painful hips? Here's the cost of arthroplasty surgery. https://www.comparehero.my/loans/articles/weak-knees-painful-hips-heres-the-cost-of-arthroplasty-surgery (2022)
- [2] M.Z. Ibrahim, A.A. Sarhan, F. Yusuf, M. Hamdi, Biomedical materials and techniques to improve the tribological, mechanical and biomedical properties of orthopedic implants—A review, J. Alloys Compd. 714 (2017) 636–667.
- [3] A. Farrahnoor, H. Zuhailawati, Review on the mechanical properties and biocompatibility of titanium implant: The role of niobium alloying element, Int. J. Mater. Res. 112(6) (2021) 505-513.

- [4] S.M. Castillo, S. Muñoz, P. Trueba, E. Díaz, Y. Torres, Influence of the compaction pressure and sintering temperature on the mechanical properties of porous, Metals 9 (2019) 1-15.
- [5] D. Mostafa, M. Aboushelib, Bioactive–hybrid–zirconia implant surface for enhancing osseointegration: an in vivo study, Int. J. Implant. Dent. 4 (2018) 1-7.
- [6] A. Farrahnoor, H. Zuhailawati, Effects of hydroxyapatite addition on the bioactivity of Ti-Nb alloy matrix composite fabricated via powder metallurgy process, Mater. Today Commun. 27 (2021) 102209.
- [7] X. Yin, C. Liang, F. Ge, Electrodeposition of a YSZ-yttria stabilized zirconia composite coating on a titanium bone implant, Int. J. Electrochem. Sci. 13 (2018) 822 831.
- [8] B.-Y. Chou, E. Chang, Plasma-sprayed hydroxyapatite coating on titanium alloy with ZrO₂ second phase and ZrO₂ intermediate layer, Surf. Coat. Technol. 153(1) (2002) 84–92.
- [9] L. Fu, K.A. Khor, J.P. Lim, Effects of yttria stabilized zirconia on plasma sprayed hydroxyapatite/yttria stabilized zirconia composite coatings, J. Am. Ceram. Soc. 85(4) (2002) 800–806.
- [10] L.L Hench, An introduction to bioceramics" 2nd edition, World Scientific, 2013.
- [11] R.M.D. Zebaze, A. Ghasem-Zadeh, A. Bohte, S. Iuliano-Burns, M. Mirams, R.I. Price, E.J. Mackie, E. Seeman, Intracortical remodelling and porosity in the distal radius and post-mortem femurs of women: A cross-sectional study, Lancet 375 (9727) (2010) 1729–1736.
- [12] A.C. Abraham, A. Agarwalla, A. Yadavalli, C. McAndrew, J.Y. Liu, S.Y. Tang, Multiscale predictors of femoral neck in situ strength in aging women: Contributions of bmd, cortical porosity, reference point indentation, and nonenzymatic glycation, JBMR 30(12) (2015) 2207–2214.
- [13] H.H. Bayraktar, E.F. Morgan, G.L. Niebur, G.E. Morris, E.K. Wong, T.M. Keaveny, Comparison of the elastic and yield properties of human femoral trabecular and cortical bone tissue, J. Biomech. 37(1) (2004) 27–35.
- [14] K. Essa, P. Jamshidi, J. Zou, M.M. Attallah, H. Hassanin, Porosity control in 316l stainless steel using cold and hot isostatic pressing, Mater. Des.138 (2018) 21-29.
- [15] M. Gradzka-Dahlke, Analysis of the processes occurring during compression of the porous 316L steel for biomedical applications, Maint. Reliab. 4 (2010) 16–22.
- [16] C.E. Wen, M. Mabuchi, Y. Yamada, K. Shimojima, Y. Chino, T. Asahina, Processing of biocompatible porous Ti and Mg, Scripta Mater. 45 (2001) 1147-1153.
- [17] L.M. Rodriguez-Albelo, P. Navarro, F.J. Gotor, J.E. de la Rosa, D. Mena, F.J. García- García, A.M. Beltrán, A. Alcudia, Y. Torres, Limits of powder metallurgy to fabricate porous Ti35Nb7Zr5Ta samples for cortical bone replacements, J. Mater. Res. Technol. 24 (2023) 6212-6226.
- [18] W.Zhang, L. Li, J. Gao, J. Huang, X. Zhang, The effect of porosity on mechanical properties of porous FeCrN stainless steel, J. Phys. Conf. Ser. 2044 (2021) 012002.
- [19] J. Zhua, D. Tanga, Z. Lua, Z. Xina, J. Songa, J. Menga, J.R. Lub, Z. Lic, J. Lia, Ultrafast bone-like apatite formation on highly porous poly(L-lactic acid)- hydroxyapatite fibres, Mater. Sci. Eng. C, 6 (2020) 111168.
- [20] S. Sakipov, A.I. Sobolevsky, M.G. Kurnikova, Ion permeation mechanism in epithelial calcium channel TRVP6 Sci. Rep. 8 (2018) 1-13.
- [21] M. Zengdong, Z. Bin, Z. Yanan, L. Lilin, Z. Yuqin, Mechanical properties and biocompatibility of porous ZnO/hydroxyapatite composites with different porosities, Chin. J. Tissue Eng. Res. 26(12) (2022) 3498-3504.